IEEE Access
Multidisciplinary | Rapid Review | Open Access Journal

Received June 28, 2019, accepted July 12, 2019, date of publication July 23, 2019, date of current version August 9, 2019.

Digital Object Identifier 10.1109/ACCESS.2019.2930567

General Theory of Skyhook Control and Its Application to Semi-Active Suspension Control Strategy Design

CHANGNING LIU[1], LONG CHEN[2], XIAOFENG YANG[1], XIAOLIANG ZHANG[2], AND YI YANG[1]
[1]School of Automotive and Traffic Engineering, Jiangsu University, Zhenjiang 212013, China
[2]Automotive Engineering Research Institute, Jiangsu University, Zhenjiang 212013, China

Corresponding author: Long Chen (chenlong@ujs.edu.cn)

This work was supported in part by the National Natural Science Foundation of China under Grant 51875257 and Grant 51705209, in part by the Natural Science Foundation of Jiangsu Province under Grant BK20160533, and in part by the Postgraduate Education Reform Project of Jiangsu Province under Grant KYCX18_2228.

ABSTRACT A novel general theory of skyhook control is proposed and applied to the semi-active suspension control strategy design to improve the performance of the vehicle suspension system. Based on this theory, the mechanical impedance model of the general theory of skyhook suspension is established. To design the suspension structure, the effect of the skyhook element and its parameters on suspension is analyzed. Then, adaptive fish swarm algorithm based on nonlinear dynamic visual field is used to optimize the parameters of the general theory of skyhook control. To realize the general theory of skyhook control and verify it, a novel controllable inerter is designed and utilized into the semi-active suspension system. The simulation results demonstrate that the semi-active suspension with a general theory of skyhook control can enhance the suspension performance. Finally, the robustness of the general theory of skyhook control under different spring stiffness and sprung mass is researched. The results indicate that the suspension with the general theory of skyhook control has superior performance and robustness compared with the traditional skyhook damper controlled suspension and passive suspension.

INDEX TERMS Semi-active suspension, skyhook control, mechanical impedance, controllable inerter.

I. INTRODUCTION

The function of vehicle suspension is to improve the ride comfort and driving safety. Today the most widely used suspension is passive suspension. It consists of spring, damper, and inerter [1]–[3]. A common approach used to design the passive suspension is structure approach [4], [5], which bases on the passive elements (spring, damper, and inerter) connected in parallel or in series. This approach can limit the complexity of the suspension structure. Whereas, some excellent structures maybe be ignored as a consequence. To solve this problem, in [1], [6], mechanical impedance approach was used into suspension design. In this approach, a mechanical impedance function is established first. Then, the parameters of mechanical impedance function are optimized based on the design objective. After that, network synthesis is used to realize the suspension structure passively. It is a more general approach compare with the structure approach. However, those two design approaches, are all obtained a fixed structure and parameters of the suspension. Normally it cannot gain the satisfying performance in all of those three indexes or must rely on a complex structure [7], [8]. Semi-active suspension can adjust suspension parameters according to the control strategy to achieve satisfying performance in different condition of the vehicle and the road [9]–[11]. Skyhook (SH) control suspension is a semi-active suspension which is easy to implement with little information about the vehicle state. It sets a virtually damper between the vehicle body and the imaginary sky [12]. It is effective to enhance the ride comfort of the vehicle, but the dynamic tire load deteriorates at the same time. In [13], a solution was proposed to improve the performance of the skyhook control strategy by adding the sliding mode and internal model theory. In term of the performance of suspension, this solution is more superior to the traditional skyhook controller. In [14], Hu and Chen designed a comfort-oriented vehicle suspension with skyhook inerter. Semi-active inerter was used to realize the semi-active skyhook inerter control and three different control laws

The associate editor coordinating the review of this manuscript and approving it for publication was Luigi Biagiotti.

were compared. It is a meaningful exploration for applying inerter to skyhook control strategy. However, those skyhook control strategies contain only one element. That is to say, the mechanical characteristics of these strategies are incomplete. From the point of mechanical network, those skyhook strategies can be seen as different kinds of special theory of skyhook control and missing some mechanical characteristic, for instance, the spring characteristic, damping characteristic, or inerter characteristic. Further improvement in suspension performance is limited.

In this paper, the problem of lacking of stiffness, damping, or inertial characteristic in skyhook control is solved and a novel general theory of skyhook (GSH) control based on the theory of mechanical impedance is proposed. In section 2, the suspension model of GSH suspension is analyzed and the transfer function of the GSH suspension is deduced. Then, the effect of the skyhook spring, skyhook damper and skyhook inerter on suspension is analyzed. The GSH control suspension structure is designed and parameters are optimized by adaptive fish swarm algorithm based on nonlinear dynamic visual field. In section 3, the semi-active suspension system based on GSH control is designed and performance is analyzed. A novel controllable inerter is proposed and devised to realize the GSH control. And random-input test is taken to evaluate the performance of the semi-active suspension based on the GSH control. Lastly, the robustness of the GSH control is analyzed with the variation in spring stiffness and sprung mass. There are two significant contributions in this paper: (1) the GSH control completes the mechanical characteristics of the skyhook control and further improves the suspension performance; (2) the novel controllable inerter proposed in this paper realizes the continuous skyhook inerter control and makes the GSH control realizable.

II. SUSPENSION DESIGN BASED ON GSH CONTROL

A. QUARTER-CAR KINETIC MODEL OF GSH CONTROL SUSPENSION

As demonstrated in Fig. 1 (a), the quarter-car kinetic model of GSH control suspension is established. It consists of a sprung mass m_2, an unsprung mass m_1, and a tire stiffness k_t. Unlike the traditional suspension model, the structure of the suspension is replaced by a mechanical impedance function $T(s)$ [15]–[17] and a virtually mechanical impedance function $Y(s)$ which is connected the skyhook and the sprung mass. In the GSH control, $Y(s)$ contains the characteristics of stiffness, damping, and inertial. So the $Y(s)$ is a general network and it can be expressed as a mechanical impedance function including springs, dampers, and inerters.

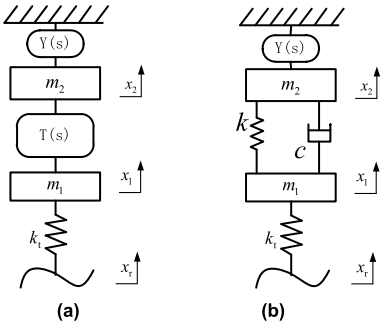

FIGURE 1. Quarter-car kinetic model. (a) GSH based on $T(s)$. (b) GSH based on traditional spring-damper structure.

The impedances of the spring, damper, and inerter have forms of k/s, c, and bs. They can be expressed in those functions as follows:

$$Y(s) = F(c_{\text{sky-i}}, \frac{k_{\text{sky-i}}}{s}, b_{\text{sky-i}}s) \tag{1}$$

$$T(s) = F(c_{\text{i}}, \frac{k_{\text{i}}}{s}, b_{\text{i}}s) \tag{2}$$

In which, $i = 1, 2, \cdots$, $k_{\text{sky-i}}$ is the i-th skyhook spring stiffness, $c_{\text{sky-i}}$ is the i-th skyhook damping coefficient, $b_{\text{sky-i}}$ is the i-th skyhook inerter coefficient, k_{i} is the i-th spring stiffness, c_{i} is the i-th damping coefficient, b_{i} is the i-th inerter coefficient.

The frequency-domain analysis of vibration transfer characteristics is convenient based on the theory of mechanical impedance. In Fig.1, m_2 is the sprung mass, m_1 is the unsprung mass, k_t is the stiffness of the tire, x_2 is the displacement of the sprung mass, x_1 is the displacement of the unsprung mass, x_r is the road random input.

Equation (3) is the dynamic model of Fig. 1 (a),

$$\begin{cases} m_2 s^2 X_2 + sT(s)(X_2 - X_1) + sY(s)X_2 = 0 \\ m_1 s^2 X_1 - sT(s)(X_2 - X_1) + k_t(X_1 - X_r) = 0 \end{cases} \tag{3}$$

In which X_2, X_1, and X_{r} are the Laplace transform of x_2, x_1, and x_{r}.

According to the Equation (3), the transfer function for body acceleration $\ddot{x}_2$ to random road input x_{r} can be deduced in (4), as shown at the bottom of this page.

The transfer function for suspension working space $x_2 - x_1$ to random road input x_{r} can be deduced in (5), as shown at the bottom of this page.

The transfer function for dynamic tire load $(x_1 - x_{\text{r}})k_{\text{t}}$ to random road input x_{r} can be deduced in (6), as shown at the bottom of the next page.

$$H_{\ddot{x}_2 \sim x_{\text{r}}}(s) = \frac{X_2}{X_{\text{r}}} s^2 = \frac{T(s)k_{\text{t}}s^3}{(m_1 m_2 s^4 + m_1 s^3(T(s) + Y(s)) + m_2 s^3 T(s) + T(s)Y(s)s^2 + k_{\text{t}} m_2 s^2 + k_{\text{t}} s(T(s) + Y(s))} \tag{4}$$

$$H_{(x_2 - x_1) \sim x_{\text{r}}}(s) = \frac{X_2 - X_1}{X_{\text{r}}} = \frac{-k_{\text{t}}(m_2 s^2 + sY(s))}{(m_1 m_2 s^4 + m_1 s^3(T(s) + Y(s)) + m_2 s^3 T(s) + T(s)Y(s)s^2 + k_{\text{t}} m_2 s^2 + k_{\text{t}} s(T(s) + Y(s))} \tag{5}$$

Select the grade-A road as input model, the pavement spectrum expressed by time frequency is

$$S(f) = \frac{G_0 u^{p-1}}{f^p} \tag{7}$$

In which, the road roughness coefficient $G_0 = 5 \times 10^{-6}$ m^3/cycle., the slope of the spectral density curve in double logarithmic coordinates $p = 2.5$, u is the speed, f is the time frequency. Setting $s = j2\pi f$, the power spectral density of the body acceleration, suspension working space, and dynamic tire load are as follows:

$$S_{\ddot{x}_2}(f) = \left|H_{\ddot{x}_2 \sim x_r}(j2\pi f)\right|^2 S(f) \tag{8}$$

$$S_{x_2 - x_1}(f) = \left|H_{(x_2 - x_1) \sim x_r}(j2\pi f)\right|^2 S(f) \tag{9}$$

$$S_{(x_1 - x_r)k_t}(f) = \left|H_{(x_1 - x_r)k_t \sim x_r}(j2\pi f)\right|^2 S(f) \tag{10}$$

The root-mean-square values are

$$BA = \sqrt{\int_0^\infty S_{\ddot{x}_2}(f)df} \tag{11}$$

$$SWS = \sqrt{\int_0^\infty S_{x_2 - x_1}(f)df} \tag{12}$$

$$DTL = \sqrt{\int_0^\infty S_{(x_1 - x_r)k_t}(f)df} \tag{13}$$

B. THE EFFECT OF STRUCTURE AND PARAMETERS ON GSH SUSPENSION

To GSH suspension, the best performance of suspension can be obtained by the appropriate structure and parameters. The high-order skyhook control strategy is always accompanied with active suspension which stands for the high cost and huge energy consumption. For the purpose of easier achievement and dependable operation, the high-order skyhook control strategy was deserted and the first-order skyhook control strategy was selected for the vehicle suspension to maintain the advantage of little control information demanded.

For the purpose of analyzing the performance of different skyhook suspension with different skyhook element separately, the suspension between the vehicle body and the tire was set as the traditional spring-damper structure. Fig. 1 (b) is the quarter-car kinetic model and $T_1(s) = k/s + c$.

To reduce the order of the suspension, $Y(s)$ was just analyzed the basic condition: one spring($Y_1(s)$), one damper($Y_2(s)$), or one inerter($Y_3(s)$). Therefore, the $Y(s)$ can be expressed as follows:

$$Y_1(s) = \frac{k_1}{s} \tag{14}$$

$$Y_2(s) = c_1 \tag{15}$$

$$Y_3(s) = b_1 s \tag{16}$$

In which, k_1 is the skyhook spring stiffness, c_1 is the skyhook damping coefficient, b_1 is the skyhook inerter coefficient. In special, when the $Y(s) = Y_2(s)$, GSH suspension is the traditional skyhook damper suspension. The GSH suspension contains the traditional skyhook damper suspension.

Select the small passenger car as the reference model. The parameters of the quarter-car kinetic model in Fig. 1 (b) are manifested in Table 1. The vehicle speed was set as 20 m/s. The time frequency $f = 0.01$.

TABLE 1. Suspension parameters.

Parameter	Values
Unsprung Mass m_1 [kg]	45
Sprung Mass m_2 [kg]	320
Spring Stiffness k [N/m]	22000
Tire Stiffness k_t [N/m]	190000
Damping Coefficient c [N·s/m]	1200

For the purpose of analyzing the effect of the one parameter of the skyhook element, suspension performance was studied with changes parameters in skyhook element. The lower and upper bounds of the parameters are demonstrated in Table 2. In which, the range of the parameter is large enough to design the vehicle suspension. And the trends of the suspension performance with the change of the parameters of skyhook element are demonstrated in Fig. 2.

TABLE 2. Range of optimized parameters.

Parameter	Lower Bound	Upper Bound
Skyhook Spring Stiffness k_1 [N/m]	0	50000
Skyhook Damping Coefficient c_1 [N·s/m]	0	20000
Skyhook Inerter Coefficient b_1 [kg]	0	5000

It is apparent from Fig. 2 that the RMS value of body acceleration, suspension working space, and dynamic tire load remain steady with the increasing of the skyhook spring stiffness k_1. The RMS value of body acceleration and dynamic tire load increases slightly (6.3%, 27.7%) and the RMS value of suspension working space decreases a little (9.2%). Therefore, the application of the skyhook spring alone has a slight impact on suspension performance. Whereas, the increase of the skyhook damping coefficient c_1 can reduce the RMS value of body acceleration and suspension working

$$H_{(x_1 - x_r)k_t \sim x_r}(s) = \frac{X_1 - X_r}{X_r} k_t = \frac{-kt(m_1 m_2 s^4 + m_1 s^3 (T(s) + Y(s)) + m_2 s^3 T(s) + T(s)Y(s)s^2)}{(m_1 m_2 s^4 + m_1 s^3 (T(s) + Y(s)) + m_2 s^3 T(s) + T(s)Y(s)s^2 + k_t m_2 s^2 + k_t s(T(s) + Y(s))} \tag{6}$$

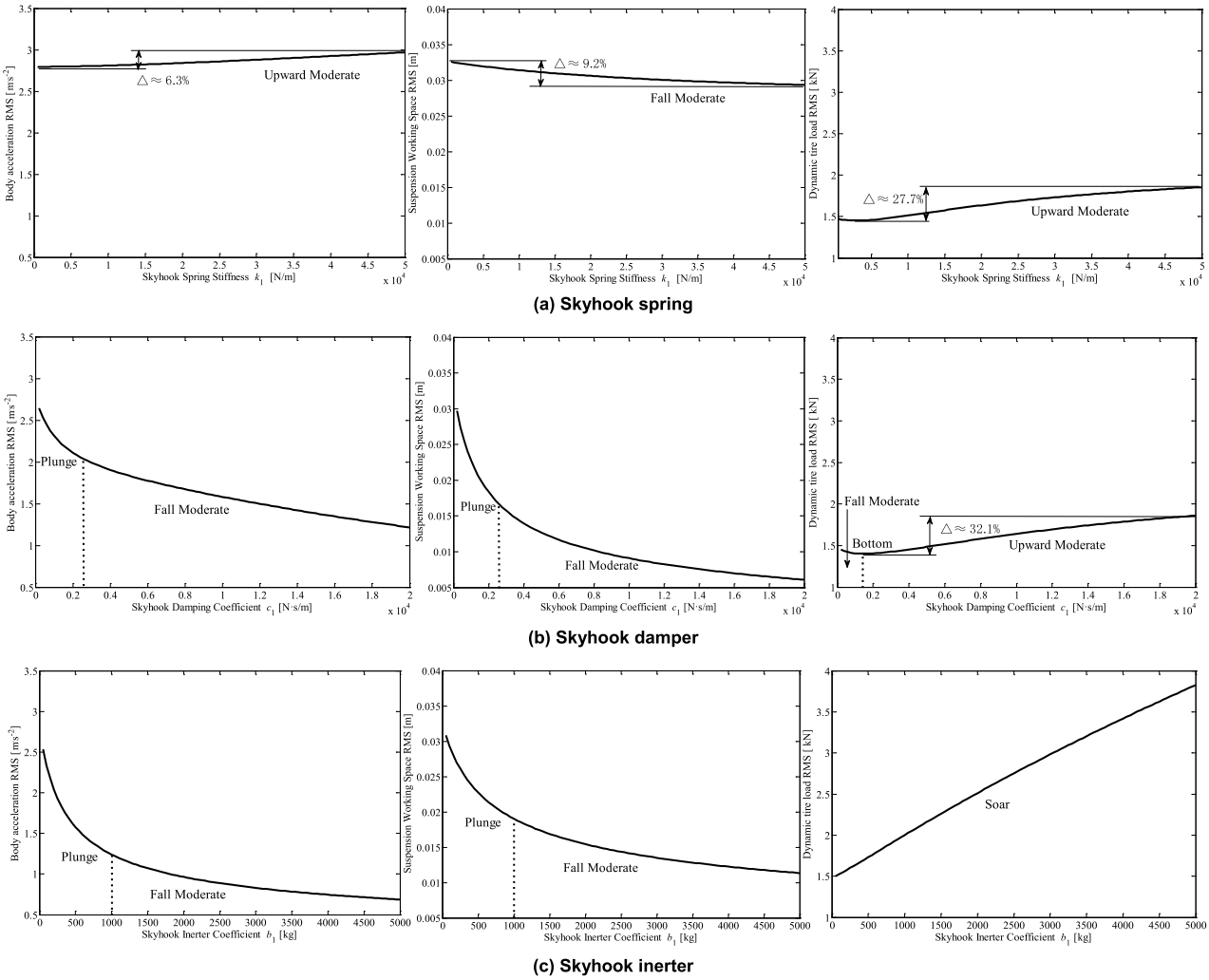

FIGURE 2. The effect of suspension performance with changes of the parameters in skyhook element.

space to some extent. When the damping coefficient c_1 is less than 2500 N · s/m, the RMS value of dynamic tire load will be reduced slightly. But when the damping coefficient is more than 2500 N · s/m, the RMS value of dynamic tire load increases a lot. And with the increase of the skyhook inerter coefficient, the RMS value of body acceleration and the suspension working space plunges. Meanwhile, the dynamic tire load soars significantly. The RMS value of body acceleration plunges when the skyhook inerter coefficient b_1 increases but less than 1000 kg. However, the suspension working space and dynamic tire load deteriorate along with the variation at the same time. So, the skyhook inerter coefficient b_1 can maintain only a small value. Because of unsatisfied performance of the skyhook spring and the key role of body acceleration in the passenger-vehicle suspension, $Y(s)$ should contain the damper characteristic and inerter characteristic. The $Y_4(s)$ is set as $c_2 + b_2 s$, in which, c_2 is the skyhook damping coefficient and b_2 is the skyhook inerter coefficient.

C. SUSPENSION PARAMETERS OPTIMIZED BY ADAPTIVE FISH SWARM ALGORITHM BASED ON NONLINEAR DYNAMIC VISUAL FIELD

Selecting the vehicle body acceleration RMS value BA, the dynamic tire load RMS value DTL, and the suspension working space RMS value SWS as the objective of ride comfort, tire grounding, and body attitude separately to design the suspension. Arranging related objective functions to find suspension parameters that focus on improving ride comfort when the RMS value of the suspension working space and dynamic tire load is not greater than the traditional suspension obviously. On account of the changing of those three indexes are different, especially the improvement of one index will cause the deterioration of other two indexes, the comprehensive evaluation index of suspension performance needs to be established. Because of the different units and orders of magnitude for body acceleration, suspension working space, and dynamic tire load, performance indexes of suspension are divided by the corresponding performance indexes of

passive suspension. The indexes of passive suspension are constant values because of the fixed parameters. This method can normalize the data of objective function. Then, they are combined by linear combination method to obtain a unified objective function:

$$\begin{aligned} \min\ F(x) &= w_1 \frac{BA}{BA_0} + w_2 \frac{SWS}{SWS_0} + w_3 \frac{DTL}{DTL_0} \\ &\Leftrightarrow \max -F(x) \\ s.t\ LB &\le x_{\mathrm{i}} \le UB \end{aligned} \tag{17}$$

where $F(x)$ is the fitness function of the adaptive fish swarm algorithm, w_1, w_2, and w_3 are the weighting coefficients and set as 0.45, 0.35, 0.2. BA_0, SWS_0, and DTL_0 are the RMS of vehicle body acceleration, suspension working space, dynamic tire load of the traditional suspension. x_{i} is decision variables. $x_{\mathrm{i}} = [c_2, b_2]$. UB is the upper bound value and LB is the lower bound value.

The skyhook damping coefficient c_2 and the skyhook inerter coefficient b_2 are optimized by adaptive fish swarm algorithm based on nonlinear dynamic visual field. And the ideal general skyhook should be realized by semi-active control strategy, which contains controllable damper and controllable inerter. To avoid the suspension damper c having an adverse effect on the optimization progress, select $T_2(s) = k/s$.

The fish swarm algorithm has strong global search ability. For the optimization of suspension parameters, the fish swarm algorithm can avoid local extrema and is not sensitive to the initial value. It is a parallel search method with high efficiency [18], [19]. However, the fixed visual field will lead the poor global search capability or poor local search ability. This paper designs an adaptive fish swarm algorithm based on nonlinear dynamic visual field. It can maintain a large visual field in the early stage to ensure the strong global search capability. As the search progresses, the visual field can adjust and the algorithm evolves into a local search, which effectively guarantees the accuracy and convergence. The visual field and moving step can be adjusted according to (18).

$$\begin{cases} Visual = Visual \times a + Visual_{\min} \\ Step = Step \times a + Step_{\min} \\ a = \exp(-30 \times (t/T_{\max})^{s}) \end{cases} \tag{18}$$

In which, s is an integer which is greater than 1, t is the current number of iterations.

The parameters range of the skyhook damping coefficient c_2 and the skyhook inerter coefficient b_2 are demonstrated in Table 3.

The vehicle speed was set as 20 m/s on a road with an unevenness coefficient of $G_0 = 5 \times 10^{-6}$ m^3/cycle. Speed white noise was selected as the road surface input. The artificial fish, with a population size of 100, the maximum number of iterations was set to 50, the maximum number of trials was 100, the initial visual field was 2.5, the congestion factor was 0.618 and the moving step was 0.3. Each artificial fish must measure the distance to the current optimal artificial fish and use it as its own visual field. The evolution of the objective function as demonstrated in Fig. 3. The optimization results of parameters in general theory of skyhook control are as follows: skyhook damping coefficient c_2 is 1897 N · s/m, skyhook inerter coefficient b_2 is 206 kg.

TABLE 3. Range of simulation parameters.

Parameter	Lower Bound	Upper Bound
Skyhook Damping Coefficient c_2 [N·s/m]	0	2500
Skyhook Inerter Coefficient b_2 [kg]	0	500

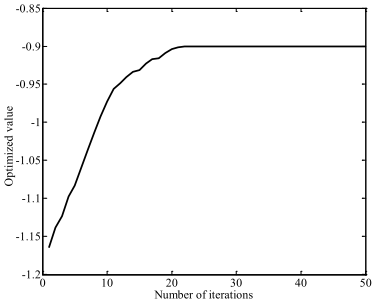

FIGURE 3. Evolution of the objective function.

III. PERFORMANCE EVALUATION OF SEMI-ACTIVE SUSPENSION SYSTEM WITH GSH CONTROL STRATEGY

A. QUARTER-CAR KINETIC MODEL OF SEMI-ACTIVE SUSPENSION

The ideal GSH suspension cannot be applied directly to engineering because the vehicle cannot be fixed to the skyhook. So the semi-active control was utilized to achieve the functions of the ideal GSH suspension. For testing the performance of the suspension, the quarter-car kinetic model of semi-active suspension based on the theory of general skyhook control was established.

As demonstrated in Fig. 4, the quarter-car kinetic model of semi-active suspension consists of the sprung mass, the unsprng mass, suspension spring, tire stiffness equivalent spring, a controllable damper and a controllable inerter. The suspension spring, controllable damper, and controllable inerter are paralleling between the sprung mass and the unsprng mass.

The kinetic equitation is

$$\begin{cases} m_1\ddot{x}_1 + k_{\mathrm{t}}(x_1 - x_r) - k(x_2 - x_1) \\ \quad -b_{ctrl}(\ddot{x}_2 - \ddot{x}_1) - c_{ctrl}(\dot{x}_2 - \dot{x}_1) = 0 \\ m_2\ddot{x}_2 + k(x_2 - x_1) + b_{ctrl}(\ddot{x}_2 - \ddot{x}_1) \\ \quad +c_{ctrl}(\dot{x}_2 - \dot{x}_1) = 0 \end{cases} \tag{19}$$

In which, m_2 is the sprung mass, m_1 is the unsprung mass, k_{t} is the stiffness of the tire, x_2 is the displacement of the

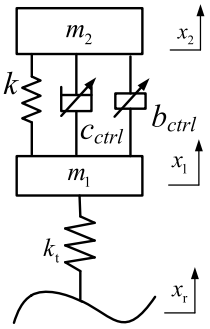

FIGURE 4. Quarter-car kinetic model of semi-active suspension.

sprung mass,x_1 is the displacement of the unsprung mass, x_r is the road random input. c_{ctrl} and b_{ctrl} are the controllable damping coefficient and the controllable inerter coefficient.

B. DESIGN OF A NOVEL CONTROLLABLE INERTER

For realizing the force of skyhook damper, there are two types of skyhook control strategy for skyhook damper: the on-off skyhook control strategy and the continuous skyhook control strategy [20]–[22]. Similarly, the skyhook inerter control strategy can be also divided into two types as above. The coefficient c_{ctrl}orb_{ctrl} has two states in the on-off skyhook control: an on-state with a maximal coefficient c_{max} or b_{max}, and an off-state with a minimal coefficient c_{min} or b_{min}. However, because the coefficient will switch between the maximal and minimal value, the control will have severe chatter problems in practice. Compared with the on-off skyhook control strategy, the continuous skyhook control strategy is closer to the ideal skyhook. It has a continuous value between the maximal and minimal coefficient of the damper or inerter.

There are a multitude of approaches to realize the continuous skyhook damper control [23]. Unlike the damper, continuous skyhook control inerter is rarely. In this paper, a novel controllable inerter was designed as manifested in Fig. 5(a) to realize the continuous skyhook inerter control.

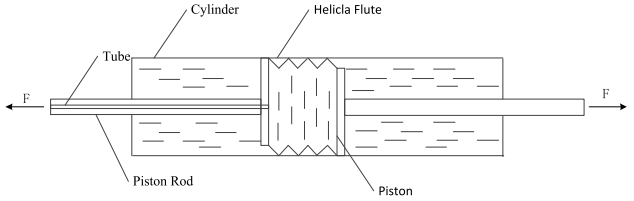

(a) The novel controllable inerter

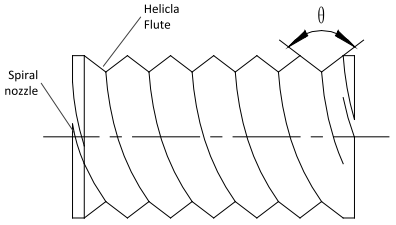

(b) Detail of controllable inerter

FIGURE 5. The structure of the novel controllable inerter.

The controllable inerter is a novel type of fluid inerter. It contains a hollow piston, two piston rods, and a cylinder. The piston is set in the cylinder. The piston rod is linked to the piston. The piston is made of hard rubber. Fig. 5(b) is its detail. It has a helical channel surrounding its outer surface. The piston and cylinder are all filled with a fluid separately. In the piston rod, there is a tube which can import or export fluid inside the piston. The cross-section of the helical channel can be viewed as an isosceles triangle. When the fluid imports or exports into the piston, the angle θ will be changed.

Excluding the nonlinearity factor, the inertia force F is the equal and opposite force applied to the terminals, x is the relative displacement between them and b is the inerter coefficient. The inertia force is described by the following equation:

$$F = b\ddot{x} \tag{20}$$

Let r_1 be the radius of the cylinder, r_2 be the radius of the piston rod, r_h be the radius of the helical channel, P_h be the pitch of the helix, and l_d be the width of the piston. l be the channel length, $l = \frac{\sqrt{P_h^2+(2\pi r_h)^2}}{P_h}$. Let a be the length of the two waists. Let S_1 be the annular area of the cylinder and ρ be the fluid density. $S_1 = \pi r_1^2$ Let S_2 be the channel cross-sectional area, $S_2 = 1/2a^2 \sin\theta$, $S_2 \in (0, 0.5a^2]$. S_3 be the cross-sectional area of the piston rod and $S_3 = \pi r_3^2$. The working area of the piston face is $(S_1 - S_3)$.

Thus, the controllable inerter coefficient b is:

$$\begin{aligned} b &= \rho \cdot l \cdot \frac{(S_1 - S_3)^2}{S_2^2} \\ &= \rho \cdot \frac{l_d\sqrt{P_h^2 + (2\pi r_h)^2}}{P_h} \cdot (\frac{2\pi(r_1 - r_3)^2}{\frac{1}{2} \cdot a^2 \cdot \sin\theta})^2 \end{aligned} \tag{21}$$

b is a coefficient relates to the θ.

The parameter of control strategy c_{ctrl} and b_{ctrl} [14] are as follows, in which, the max value of c_{max} is c_2, the max value of b_{max} is b_2, and the ideal value of c_{min} and b_{min} are zero.

$$c_{ctrl} = \begin{cases} \max(c_{min}, \min(\frac{c_{sky}\dot{x}_2}{\dot{x}_2 - \dot{x}_1}, c_{max}, & \dot{x}_2(\dot{x}_2 - \dot{x}_1) \geq 0 \\ c_{min}, & \dot{x}_2(\dot{x}_2 - \dot{x}_1) < 0 \end{cases} \tag{22}$$

$$b_{ctrl} = \begin{cases} \max(b_{min}, \min(\frac{b_{sky}\ddot{x}_2}{\ddot{x}_2 - \ddot{x}_1}, b_{max}, & \ddot{x}_2(\ddot{x}_2 - \ddot{x}_1) \geq 0 \\ b_{min}, & \ddot{x}_2(\ddot{x}_2 - \ddot{x}_1) < 0 \end{cases} \tag{23}$$

C. TEST IN RANDOM INPUT

Integral white noise of time-domain expression is taken as the road input, the input equation is:

$$\dot{x}_r(t) = 2\pi\sqrt{G_0 u}w(t) \tag{24}$$

In which $\boldsymbol{w(t)}$ is a mean value of zero Gauss white noise, G_0 is the road roughness coefficient, u is the vehicle speed.

In this test, the vehicle speed u was 20 m/s and the road roughness coefficient G_0 was $\times 10^{-6}$ m^3/cycle. To analyze the performance of those GSH controlled suspension, the traditional spring-damper structure suspension and the traditional skyhook damper control suspension (SH control suspension) were used as the comparative target and the random road information was taken as input of it. The parameters of the traditional suspension are $k_0 = 22000$ N/m, $c_0 = 1200$ N·s/m. The skyhook damper coefficient of the SH control suspension $c_{sky0} = 1897$ N · s/m. Other parameters are same as the traditional suspension. It is a special situation of GSH control suspension when the b_{ctrl} is set to 0. The system output power spectral density of random response manifested in Fig. 6. The RMS values of the three indexes were demonstrated in Table 4.

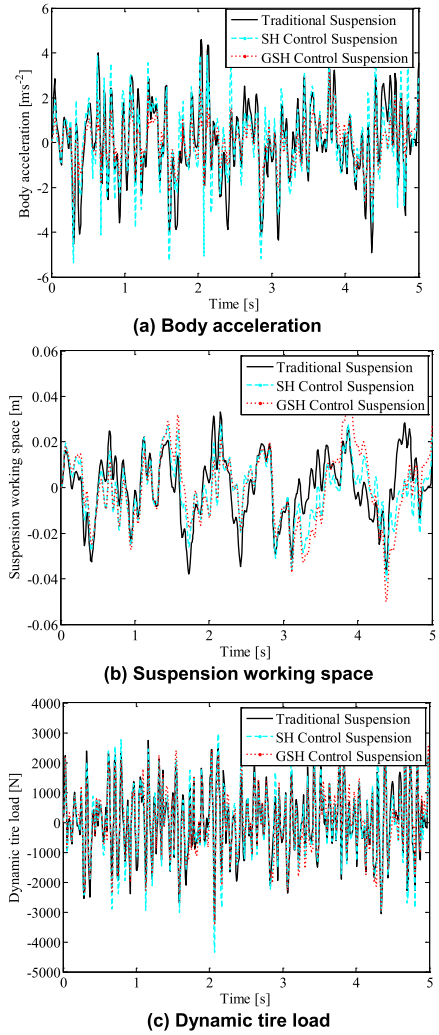

FIGURE 6. Comparison of three types suspensions.

As demonstrated in Fig. 6, select the performance of the passive suspension and SH control suspension as the standard reference, the body acceleration and dynamic tire load of the GSH control suspension decrease a lot. The suspension working space increases a little. But when the suspension working space within a reasonable range, the suspension can absorb road vibration and avoid vibration transmit to the vehicle body. Therefore, the suspension with GSH control has better performance of body acceleration and dynamic tire load compared with the passive suspension and suspension with SH control. To quantify the performance of the suspension with GSH control, the RMS value of the three performance indexes and the percentage of the improvement comparing with the passive suspension are recorded in Table 4. The positive variation number means the value is increased, and the performance is deteriorated. The negative variation number means the value is decreased, and the performance is enhanced. Clearly, the suspension with SH control improves the performance of body acceleration (−5.6%) at the cost of deteriorated performance in dynamic tire load (+7.9%). Whereas, the GSH controlled suspension avoids this disadvantage. The body acceleration decreases approximately 45.4% and the dynamic tire load decreases approximately 4.2%. The Fig. 6 and Table 4 indicate that the semi-active suspension based on the GSH control improves the suspension performance significantly.

D. INFLUENCES OF SPRING STIFFNESS AND SPRUNG MASS ON SUSPENSION PERFORMANCE

The spring stiffness k and sprung mass m_2 have a considerable effect on the performance of suspension. In addition, the sprung mass m_2 is variable during different conditions such as the empty loaded condition and the fully loaded condition. For the purpose of further exploration of the robustness of the GSH controlled suspension performance under different working conditions, the spring stiffness k and sprung mass m_2 were set to different values, and the suspension model was simulated.

The value of the spring stiffness k is defined in percentage changes from the initially value given in Table 1. The variations range of the spring stiffness was from 50% descent to 50% ascent. There are two conditions of the sprung mass m_2: the empty loaded condition ($m_2 = 320$ kg) and the fully loaded condition ($m_2 = 450$ kg).

The simulation results are manifested in Fig. 7. For all of those three suspensions, the fully loaded condition has small RMS value in body acceleration and larger RMS value in dynamic tire load comparing with the empty loaded condition. With the alteration of the spring stiffness k and sprung mass m_2, performance indexes of GSH controlled suspension are all small than the passive suspension in the case of the same spring stiffness and sprung mass. In addition, the fluctuation of those indexes of GSH controlled suspension is smaller than the passive suspension and the SH controlled suspension, except the little increase of the dynamic tire load. But as a small passenger car, the variation of the dynamic tire load has a little effect on the road. For the robustness, the increase of the RMS value of body acceleration for GSH and SH control suspension is about 50%, but about 105% for passive suspension.

TABLE 4. RMS values and its variation of random response outputs.

Performance Index	Traditional Suspension	SH Control Suspension	Variation	GSH Control Suspension	Variation
Body Acceleration RMS [$m \cdot s^{-2}$]	1.7623	1.6683	-5.6%	0.9617	-45.4%
Suspension Working Space RMS [m]	0.0147	0.0128	-12.9%	0.0157	6.8%
Dynamic Tire Load RMS [kN]	1.1700	1.2628	7.9%	1.1214	-4.2%

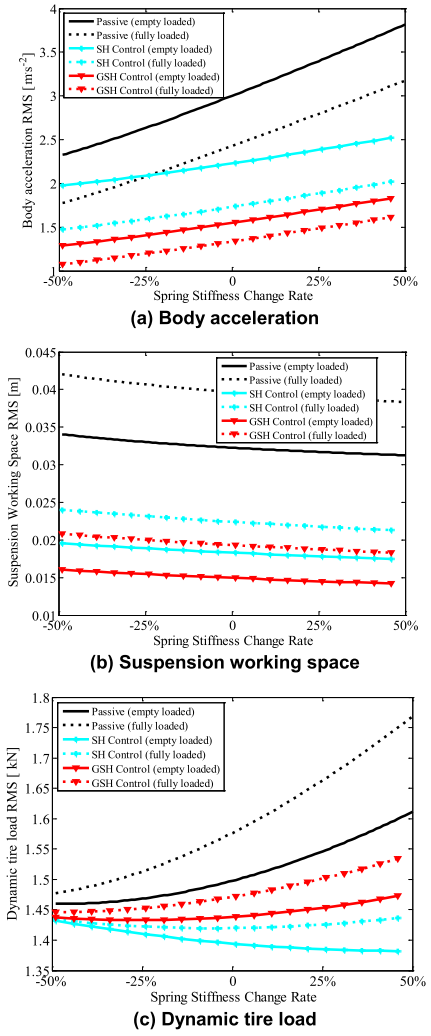

FIGURE 7. Influences of spring stiffness and sprung mass on vehicle performance.

In general, the GSH controlled suspension has superior performance and robustness in different working conditions. With the changing of the spring stiffness and the sprung mass, the GSH controlled suspension has better robustness than the passive suspension and the SH controlled suspension.

IV. CONCLUSION

This paper proposed a novel general theory of skyhook control and designed a novel controllable inerter which can realize the continuous skyhook inerter control strategy. It promoted the special theory of skyhook control at present. The testing results demonstrated that the suspension applied GSH control strategy can enhance the suspension performance obviously. What's more, the analysis of the influence of spring stiffness and sprung mass on suspension performance demonstrated that under different working conditions, the GSH control suspension had superior performance and robustness compared with the traditional skyhook control suspension and passive suspension. The significance of the general skyhook control strategy and the novel controllable inerter can be concluded as:

1. The application of the GSH control strategy into vehicle suspension can obtain superior suspension performance, especially in indexes of the body acceleration (improve 45.4%) and dynamic tire load (improve 4.2%) compare with the passive suspension. And with the changing of the spring stiffness (±50%) and the sprung mass (empty loaded or fully loaded), the GSH controlled suspension had better robustness than the passive suspension and the SH controlled suspension. It extends new ideas for suspension control.
2. The paper applied the transfer function to designing the control strategy and explored the effect of the skyhook spring, skyhook damper, and skyhook inerter on suspension. According to the analysis results, the structure of suspension was designed and the parameters were optimized by adaptive fish swarm algorithm based on nonlinear dynamic visual field. This approach can be utilized into a more complex structure GSH suspension system.
3. A novel controllable inerter was designed to realize the continuous skyhook inerter control strategy. It is the foundation of the GSH suspension and has a significance value in the engineering of the controllable inerter.

ACKNOWLEDGMENT

The authors would like to thank the associate editor and the anonymous reviewers for their careful reading and helpful comments.

REFERENCES

[1] M. C. Smith, "Synthesis of mechanical networks: The inerter," *IEEE Trans. Autom. Control*, vol. 47, no. 10, pp. 1648–1662, Oct. 2002.

[2] J.-Y. Li and S. Zhu, "Versatile behaviors of electromagnetic shunt damper with a negative impedance converter," *IEEE/ASME Trans. Mechatronics*, vol. 23, no. 3, pp. 1415–1424, Jun. 2018.

[3] X. Wang, X. Liu, Y. Shan, Y. Shen, and T. He, "Analysis and optimization of the novel inerter-based dynamic vibration absorbers," *IEEE Access*, vol. 6, pp. 33169–33182, 2018.

[4] F. Scheibe and M. C. Smith, "Analytical solutions for optimal ride comfort and tyre grip for passive vehicle suspensions," *Vehicle Syst. Dyn.*, vol. 47, no. 10, pp. 1229–1252, Oct. 2009.
[5] Y. Hu, M. Z. Q. Chen, Z. Shu, and L. Huang, "Analysis and optimisation for inerter-based isolators via fixed-point theory and algebraic solution," *J. Sound Vib.*, vol. 346, pp. 17–36, Jun. 2015.
[6] C. Papageorgiou and M. C. Smith, "Positive real synthesis using matrix inequalities for mechanical networks: Application to vehicle suspension," *IEEE Trans. Control Syst. Technol.*, vol. 14, no. 3, pp. 423–435, May 2006.
[7] M. Z. Q. Chen, K. Wang, Y. Zou, and G. Chen, "Realization of three-port spring networks with inerter for effective mechanical control," *IEEE Trans. Autom. Control*, vol. 60, no. 10, pp. 2722–2727, Oct. 2015.
[8] K. Wang, M. Z. Q. Chen, and Y. Hu, "Synthesis of biquadratic impedances with at most four passive elements," *J. Franklin Inst.*, vol. 351, no. 3, pp. 1251–1267, Mar. 2014.
[9] X. Ma, P. K. Wong, J. Zhao, J.-H. Zhong, H. Ying, and X. Xu, "Design and testing of a nonlinear model predictive controller for ride height control of automotive semi-Active air suspension systems," *IEEE Access*, vol. 6, pp. 63777–63793, 2018.
[10] X. Tang, H. Du, S. Sun, D. Ning, Z. Xing, and W. Li, "Takagi–Sugeno fuzzy control for semi-active vehicle suspension with a magnetorheological damper and experimental validation," *IEEE/ASME Trans. Mechatronics*, vol. 22, no. 1, pp. 291–300, Feb. 2017.
[11] M. Z. Q. Chen, Y. Hu, C. Li, and G. Chen, "Application of semi-Active inerter in semi-active suspensions via force tracking," *J. Vib. Acoust.*, vol. 138, no. 4, pp. 1–11, Aug. 2016.
[12] D. Karnopp, M. J. Crosby, and R. A. Harwood, "Vibration control using semi-Active force generators," *J. Eng. Ind.*, vol. 96, no. 2, pp. 619–626, May 1974.
[13] A. Jayabalan and N. K. S. Kumar, "Vibration suppression of quarter car using sliding-mode and internal model-based skyhook controller," *J. Vib. Eng. Technol.*, vol. 6, no. 2, pp. 117–126, Jun. 2018.
[14] Y. Hu, M. Z. Q. Chen, and Y. Sun, "Comfort-oriented vehicle suspension design with skyhook inerter configuration," *J. Sound Vib.*, vol. 405, pp. 34–47, Sep. 2017.
[15] M. C. Smith and F.-C. Wang, "Performance benefits in passive vehicle suspensions employing inerters," in *Proc. 42nd IEEE Int. Conf. Decis. Control*, Dec. 2003, pp. 2258–2263.
[16] M. Z. Q. Chen and M. C. Smith, "Restricted complexity network realizations for passive mechanical control," *IEEE Trans. Autom. Control*, vol. 54, no. 10, pp. 2290–2301, Oct. 2009.
[17] L. Chen, C. Liu, W. Liu, J. Nie, Y. Shen, and G. Chen, "Network synthesis and parameter optimization for vehicle suspension with inerter," *Adv. Mech. Eng.*, vol. 9, no. 1, pp. 1–7, Jan. 2016.
[18] W. Zhao, C. Du, and S. Jiang, "An adaptive multiscale approach for identifying multiple flaws based on XFEM and a discrete artificial fish swarm algorithm," *Comput. Methods Appl. Mech. Eng.*, vol. 339, pp. 341–357, Sep. 2018.
[19] A. M. A. C. Rocha, M. F. P. Costa, and E. M. G. P. Fernandes, "A shifted hyperbolic augmented Lagrangian-based artificial fish two-swarm algorithm with guaranteed convergence for constrained global optimization," *Eng. Optim.*, vol. 48, no. 12, pp. 2114–2140, Apr. 2016.
[20] A. C. Zolotas and R. M. Goodall, "New insights from fractional order skyhook damping control for railway vehicles," *Vehicle Syst. Dyn.*, vol. 56, no. 11, pp. 1–24, Feb. 2018.
[21] C.-Y. Hsieh, B. Huang, F. Golnaraghi, and M. Moallem, "Regenerative skyhook control for an electromechanical suspension system using a switch-mode rectifier," *IEEE Trans. Veh. Technol.*, vol. 65, no. 12, pp. 9642–9650, Dec. 2016.
[22] S. B. A. Kashem, M. Ektesabi, and R. Nagarajah, "Comparison between different sets of suspension parameters and introduction of new modified skyhook control strategy incorporating varying road condition," *Vehicle Syst. Dyn.*, vol. 50, no. 7, pp. 1173–1190, Jul. 2012.
[23] A. Shamsi and N. Choupani, "Continuous and discontinuous shock absorber control through skyhook strategy in semi-active suspension system (4DOF model," *Int. J. Mech., Ind. Aerosp. Eng.*, vol. 2, no. 5, pp. 697–701, 2008.

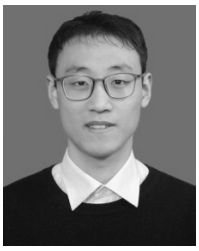

CHANGNING LIU is currently pursuing the Ph.D. degree with the School of Automotive and Traffic Engineering, Jiangsu University, China. His main research interests include the dynamic modeling and control of vehicle suspension, especially the structure design, performance evaluation, and active/semi-active control of the ISD (inerter-spring-damper) suspension.

LONG CHEN is currently a Professor with the Research Institute of Automotive Engineering, Jiangsu University, China. His main research interests include the dynamic modeling and control of vehicle engineering.

XIAOFENG YANG is currently an Associate Professor with the School of Automotive and Traffic Engineering, Jiangsu University, China. His main research interests include the dynamic modeling and control of vehicle engineering.

XIAOLIANG ZHANG is currently a Professor with the Research Institute of Automotive Engineering, Jiangsu University, China. His main research interests include the dynamic modeling and control of vehicle engineering.

YI YANG is currently pursuing the Ph.D. degree with the School of Automotive and Traffic Engineering, Jiangsu University, China. Her main research interests include the dynamic modeling and control of vehicle suspension, especially the structure design, performance evaluation, and active/semi-active control of the ISD (inerter-spring-damper) suspension.